A&A 486, 837–841 (2008)
DOI: 10.1051/0004-6361:200809669

Astronomy & Astrophysics

Non-thermal bremsstrahlung from supernova remnants and the effect of Coulomb losses *(Research Note)*

Jacco Vink

Astronomical Institute Utrecht, Utrecht University, PO Box 80000 3508TA, Utrecht, The Netherlands
e-mail: j.vink@astro.uu.nl

Received 27 February 2008 / Accepted 28 May 2008

ABSTRACT

Aims. We investigate the shape of the electron cosmic ray spectrum in the range up to ∼1000 keV, assuming that the acceleration process at the shock results in a power law in momentum, and that downstream of the shock the spectrum is affected by Coulomb interactions with background electrons only.
Methods. In the non-relativistic regime one can analytically determine the energy of an electron starting with a certain energy, and use this result to produce an electron cosmic ray spectrum, modified by Coulomb losses.
Results. An analytic expression for the electron spectrum is obtained that depends on the parameter $n_e t$, which can be estimated from a similar parameter used to characterize the line spectra of supernova remnants.
Conclusions. For the brightest supernova remnants $n_e t > 10^{11}$ cm^{-3} s, and most of the electrons accelerated to <100 keV have lost their energy. Because of its high radio flux, Cas A is the most likely candidate for non-thermal bremsstrahlung. Although it has $n_e t \sim 2 \times 10^{11}$ cm^{-3} s, one may expect to pick up non-thermal bremsstrahlung above 100 keV with current hard X-ray detectors.

Key words. ISM: cosmic rays – acceleration of particles – ISM: supernova remnants – X-rays: ISM – shock waves – radiation mechanisms: non-thermal

1. Introduction

Over the last five years there has been considerable progress in our understanding of high energy cosmic ray acceleration by supernova remnants (SNRs). The spatial distribution and spectral shape of X-ray synchrotron emission from all historical SNRs and some other SNRs has made it clear that electron can be accelerated to energies up to ∼100 TeV (Koyama et al. 1995), that diffusive shock acceleration works very efficiently, with diffusion close to the Bohm limit (Vink 2005; Vink et al. 2006; Parizot et al. 2006; Stage et al. 2006), and that magnetic fields are amplified by cosmic ray streaming (Vink & Laming 2003; Berezhko et al. 2003; Bamba et al. 2005; Völk et al. 2005). Moreover, the morphology of Tycho's SNR shows that at least in this remnant, but also probably in Kepler's SNR, cosmic ray acceleration is so efficient that it gives rise to enhanced compression ratios (Warren et al. 2005; Ellison et al. 2004). In addition, considerable progress has been made in the field of TeV astronomy, with many SNRs being established as sources of TeV γ-rays (e.g. Aharonian et al. 2004, 2005; Albert et al. 2007). However, it has not yet been firmly established whether the γ-ray emission is dominated by inverse Compton scattering from TeV electrons, or from neutral pion decay, caused by TeV ion cosmic rays.

In contrast, little has happened concerning observations of low energy cosmic rays. This is unfortunate, since from a theoretical perspective, the initial stages of the acceleration process, from thermal energies up to energies where Fermi acceleration efficiently operates, is complex and not well understood (see e.g. Malkov & Drury 2001, for a review). In fact, the processes by which particles are injected into the Fermi acceleration process, are likely to be different for electrons and ions, unlike Fermi acceleration itself. Our current understanding of the initial stages of acceleration is largely based on either in situ observations of inter-planetary shocks, and on computer modeling using hybrid or particle in cell codes (e.g. Bykov & Uvarov 1999; Schmitz et al. 2002; Lee et al. 2004). There was some hope that hard X-ray observations of SNRs might provide observational information on at least the electron component of low energy cosmic rays (Asvarov et al. 1990; Favata et al. 1997; Vink et al. 1997; Vink & Laming 2003). However, it is generally agreed that the non-thermal hard X-ray emission from SNRs such as Cas A (The et al. 1996; Allen et al. 1997; Favata et al. 1997; Vink & Laming 2003; Renaud et al. 2006b), SN1006 (Allen et al. 1999; Kalemci et al. 2006), Tycho (Allen et al. 1999), Kepler and RCW 86 (Allen et al. 1999) is due to X-ray synchrotron from the highest energy electron cosmic rays, rather than from bremsstrahlung from low energy electrons. Nevertheless, the issues remains of interest as current and future hard X-ray detectors push the detection of hard X-ray emission to higher photon energies. At high enough energies, the steepening X-ray synchrotron spectrum is likely to be overtaken by non-thermal bremsstrahlung.

In this paper, I discuss the shape of the low energy cosmic ray electron spectra, given the importance of Coulomb-losses. These Coulomb losses in general alter the shape of the low electron cosmic ray spectrum as generated near the shock front. Note that

a similar situation was investigated by Sarazin (1999) for higher energy electrons in clusters of galaxies.

2. Coulomb loss affected electron spectra

2.1. The electron energy as a function of time

Supra-thermal electrons loose energy through various processes: bremsstrahlung losses, Coulomb losses (collisions with electrons/ions), and ionization losses[1]. In the hot plasmas inside SNR shells Coulomb losses are likely to be the dominant source of energy losses of electrons, in particular through electron-electron collisions (e.g. Haug 2004). Electron-electron collisions are most efficient at low electron energies. For SNRs we are interested in the bremsstrahlung emission of supra-thermal electron with energies in the range of ∼10−1000 keV. The problem with this energy range is that neither the non-relativistic, nor the relativistic approximations for Coulomb losses are completely valid. However, I will show that for most SNRs the non-relativistic approximation is sufficient.

The energy loss rate for an electron with $E \gg kT_\mathrm{e}$ is given by (e.g. Haug 2004; Huba 2002):

$$\frac{\mathrm{d}E}{\mathrm{d}t} = -4\pi r_\mathrm{e}^2 m_\mathrm{e} c^3 \frac{\epsilon+1}{p} \lambda_\mathrm{ee} n_\mathrm{e}, \tag{1}$$

with r_e the classical electron radius, and ϵ and p the kinetic energy and momentum in dimensionless units, n_e the electron density, and λ_ee the Coulomb logarithm, given by (Huba 2002):

$$\lambda_\mathrm{ee} = 30.9 - \ln\left[n_\mathrm{e}^{1/2}\left(\frac{1\ \mathrm{keV}}{kT_\mathrm{e}}\right)\right]. \tag{2}$$

For the non-relativistic limit ($\epsilon \ll 1$) Eq. (1) gives:

$$\frac{\mathrm{d}E}{\mathrm{d}t} = -\frac{4\pi r_\mathrm{e}^2 m^2 c^4}{\sqrt{2m_\mathrm{e}E}} \lambda_\mathrm{ee} n_\mathrm{e} = -\frac{7.73\times10^{-6}}{\sqrt{E}} \lambda_\mathrm{ee} n_\mathrm{e}, \tag{3}$$

with energies, E in units of eV.

The solution to this differential equation is:

$$E(t) = \left(E_0^{3/2} - 1.16\times10^{-5}\lambda_\mathrm{ee} n_\mathrm{e} t\right)^{2/3}, \tag{4}$$

with E_0 the energy of the electron at $t = 0$.

In fact, the correct equation, Eq. (1), can also be solved, but only gives an implicit function for $E(t)$:

$$\begin{aligned} n_\mathrm{e}t \;=\; & \frac{\sqrt{\left(\frac{E_0}{mc^2}+1\right)^2-1} - \arctan\sqrt{\left(\frac{E_0}{mc^2}+1\right)^2-1}}{4\pi r_\mathrm{e}^2 c\lambda_\mathrm{ee}} \\ & - \frac{\sqrt{\left(\frac{E}{mc^2}+1\right)^2-1} - \arctan\sqrt{\left(\frac{E}{mc^2}+1\right)^2-1}}{4\pi r_\mathrm{e}^2 c\lambda_\mathrm{ee}}. \end{aligned} \tag{5}$$

Figure 1 shows both the full solution and the non-relativistic approximation. As expected, the non-relativistic approximation fails at high energies. For energies ≲400 keV the approximation is reasonable, with errors in the loss timescale of less than 30%.

[1] In contrast, in the GeV-TeV range the dominant losses are due to synchrotron radiation and Coulomb losses, limiting the maximum electron energy that can be obtained (e.g. Drury et al. 1999).

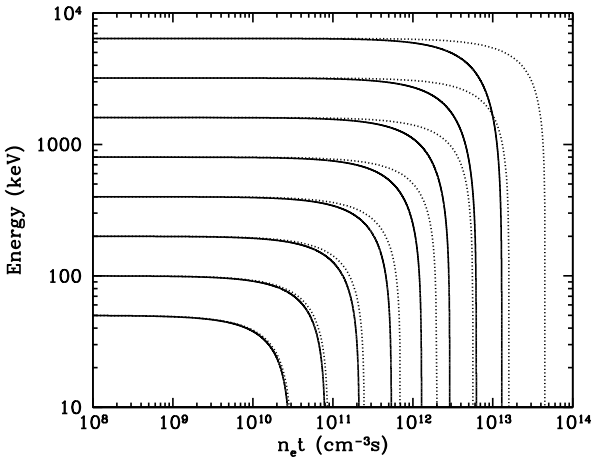

Fig. 1. The electron energy as a function of $n_\mathrm{e}t$ ($\lambda_\mathrm{ee} = 30.9$) for different values of energy at $t = 0$ s (50 keV, 100 keV, 200 keV...6400 keV). The solid lines show the exact, but implicit solutions to Eq. (1), i.e. Eq. (5). The dotted lines are the non-relativistic solutions to Eq. (1), i.e. Eq. (4).

2.2. An analytic approximation to the non-thermal spectrum

The advantage of an explicit function (Eq. (4)) is that it can be easily used to calculate the evolution of the electron spectrum, using the transformation $N(E_0) \rightarrow N(E(t))$, if an analytic approximation is known. This can be done by inverting Eq. (4) and insert the result in $N(E)$, taking into account that

$$\frac{\mathrm{d}E_0}{\mathrm{d}E} = (E^{3/2} + 1.16\times10^{-5}\lambda_\mathrm{ee} n_\mathrm{e} t)^{-1/3} E^{1/2}. \tag{6}$$

A simple example is when $N(E)$ can be approximated by a power law $N(E_0)\mathrm{d}E_0 = KE_0^{-\Gamma}\mathrm{d}E_0$. After some time t the spectrum will be approximated by:

$$N(E)\mathrm{d}E = K(E^{3/2} + 1.16\times10^{-5}\lambda_\mathrm{ee} n_\mathrm{e} t)^{-(2\Gamma+1)/3} E^{1/2}\mathrm{d}E. \tag{7}$$

A more interesting function in this context is the power law in momentum $N(p) = Kp^{-\Gamma}$, since the simplest version of first order Fermi acceleration predicts that this is the spectrum of cosmic rays. Changing this into a function of energy ($E = \sqrt{p^2c^2 + (mc^2)^2} - mc^2$) gives (see Asvarov et al. 1990):

$$N(E)\mathrm{d}E = \frac{K}{c^{-\Gamma}}(E^2 + 2Emc^2)^{-\frac{\Gamma+1}{2}} \times (E + mc^2)\mathrm{d}E. \tag{8}$$

Inserting Eqs. (4) and (6) in this expression gives:

$$\begin{aligned} N(E)\mathrm{d}E \;=\; & \frac{N_p}{c^{-\Gamma}} \times \Big((E^{3/2} + 1.16\times10^{-5}\lambda_\mathrm{ee} n_\mathrm{e} t)^{4/3} \\ & + 2mc^2(E^{3/2} + 1.16\times10^{-5}\lambda_\mathrm{ee} n_\mathrm{e} t)^{2/3}\Big)^{-(\Gamma+1)/2} \\ & \times \Big((E^{3/2} + 1.16\times10^{-5}\lambda_\mathrm{ee} n_\mathrm{e} t)^{2/3} + mc^2\Big) \\ & \times \Big(E^{3/2} + 1.16\times10^{-5}\lambda_\mathrm{ee} n_\mathrm{e} t\Big)^{-1/3} E^{1/2}\mathrm{d}E. \end{aligned} \tag{9}$$

One of the important aspects of this solution is that it depends almost entirely on one parameter $n_\mathrm{e}t$, since λ_ee only weakly depends on the plasma density and temperature. This parameter is familiar to anyone investigating X-ray emission from SNRs, as it is the key parameter for non-ionization equilibrium (NEI, see Liedahl 1999) and for the equilibration of electrons and ions. In

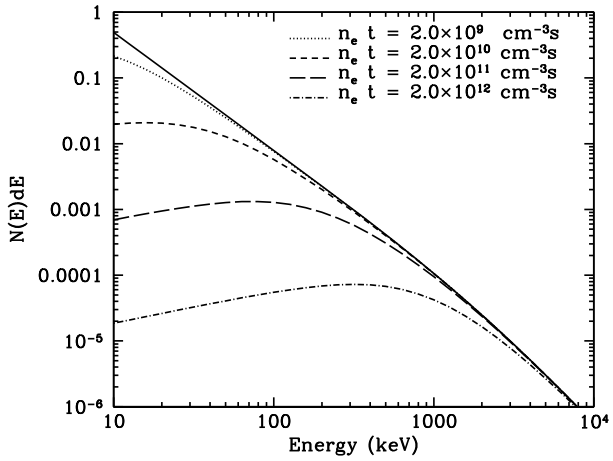

Fig. 2. Low energy electron cosmic rays as expected from first order Fermi acceleration, including the effects of Coulomb losses (Eq. (9)). The solid line gives the expected spectrum near the shock front, whereas the other lines show the models for different values of $n_e t$.

both cases the parameter is a measure for the number of collisions with background electrons.

Figure 2 shows the electron distributions for values of $n_e t$ covering the relevant range for SNRs, 10^9–10^{12} cm^{-3} s. Figure 1 shows that for young SNRs the non-relativistic approximation is expected to be valid, as large errors only appear for $n_e t \gtrsim 5 \times 10^{11}$ cm^{-3} s. Moreover, the errors mostly affect the spectral shapes above 500 keV.

3. Discussion and application to Cas A

As explained above the shape of the non-thermal electron spectrum below 1000 keV depends on the parameter $n_e t$, which is the same parameter that governs the ionization state of the SNR. However, it depends on the details of the shock acceleration history, whether one can safely assume that the average $n_e t$ of the hot plasma corresponds to the $n_e t$ governing the shape of the low energy electron cosmic rays. A close correspondence is likely if shock heating results always in a fixed ratio of heated and accelerated electrons at the shock front. Realistically, one should take into account the variation of $n_e t$ throughout the SNR, and the evolution with time. However, in practise one or two values for $n_e t$ characterizes the overall plasma characteristics reasonably well (e.g. Vink et al. 1996).

For young SNRs like Cas A, Tycho, Kepler and SN1006, the X-ray spectra are dominated by line emission from ejecta, shock heated by the reverse shock. This means that also $n_e t$ is determined mostly by the plasma heated by the reverse shock, rather than by the forward shock heated plasma. It is often assumed that the reverse shock has a low magnetic field and therefore does not efficiently accelerate cosmic rays. However, Helder & Vink (2008) showed recently that the reverse shock of Cas A is responsible for most of the X-ray synchrotron emission, this implies that the reverse shock is capable of accelerating particles as well. This is a confirmation of recent theoretical calculations by Ellison et al. (2005). Nevertheless, it is not quite clear what the ratio is of the electrons accelerated by the forward shock, as opposed to the reverse shock. Moreover, the initial acceleration process for electrons may be different: the reverse shocked plasma is dominated by metals. In that case, a sizable fraction of the accelerated electrons may originate from ionization of (mildly) accelerated ions.

Apart from the plasma $n_e t$ there is another reason why the $n_e t$ for the accelerated electrons is expected to be high in Cas A: most of the electrons seem to have been accelerated in the early life of the SNR. The best evidence for this is the ∼1%/yr decline in its radio flux, which is best explained by adiabatic expansion of the relativistic electron gas (Shklovsky 1968). Cas A may be a special case since it is evolving into a red super giant wind, which has a density falling of with radius as r^{-2}. This means that the particle flux entering the forward shock at any radius is more or less constant, whereas the shock velocity is dropping with radius. As a result particle acceleration was more efficient early on, suggesting a high $n_e t$.

Unfortunately, this also means that it is quite unlikely that the non-thermal X-ray emission of Cas A below ∼100 keV is dominated by non-thermal bremsstrahlung, either from the forward shock, or from internal shocks, as assumed by (Laming 2001a,b; Vink & Laming 2003). The reason is that all the emission must then come from a limited fraction of the total shock heated plasma for which $n_e t < 10^{10}$ cm^{-3} s (see Willingale et al. 2002; Yang et al. 2007, for the spatial distribution of $n_e t$). If I simply assume a linear relation between age and $n_e t$, less than 5% of the plasma has $n_e t < 10^{10}$ cm^{-3} s. The lower hybrid wave model propagated by Laming (2001a) remains an attractive option for the injection of electrons into the Fermi acceleration process itself (see also Ghavamian et al. 2007).

Nevertheless, Cas A remains one of the most important targets for searching for non-thermal bremsstrahlung, but only above ∼100 keV, where the spectrum is less affected by Coulomb losses. The reason is that Cas A is by far the brightest Galactic SNR in the radio. This implies the ample presence of relativistic electrons, in combination with a relatively high magnetic field of 100–500 μG (Shklovsky 1968; Vink & Laming 2003; Berezhko & Völk 2004). This is illustrated in Fig. 3, which suggests that with INTEGRAL-ISGRI we may be close to a detection, or even that part of the flux density around 100 keV is caused by non-thermal bremsstrahlung (cf. the CGRO-OSSE detection, The et al. 1996). No deep Suzaku Hard X-ray Detector (HXD) (Takahashi et al. 2007) of Cas A exist, but a deep observation with this sensitive instrument, may also be able to detect emission above 100 keV.

The normalization of the spectrum in Fig. 3 is determined from the radio flux, and assuming a mean magnetic field of ∼300 μG. The bremsstrahlung also depends on the emission measure: EM $= \int \Sigma_i n_i n_e Z_i^2 \mathrm{d}V$, with n_e being, here, the density of the accelerated electrons. For Cas A the accelerated electrons are present in both the forward shock heated plasma, with $n_H \approx 10$ cm^{-3}, and in the reverse shock heated plasma, which consists of pure metals, probably dominated by almost completely ionized oxygen (e.g. Vink et al. 1996). The emitting volume of the forward shock heated plasma is $V_f \approx 1.2 \times 10^{57}$ cm^3, based on a shock radius of 2.6 pc and a contact discontinuity at ∼2 pc. The reverse shock radius is ∼1.9 pc (Helder & Vink 2008), thus $V_r \approx 1.4 \times 10^{56}$ cm^3. Conservatively assuming that there is ∼1 $M_\odot$ of ionized oxygen (Vink et al. 1996) and that the other metals contribute little to the bremsstrahlung, one finds for the shocked ejecta $\Sigma_i n_i Z_i^2 \approx 35$ cm^{-3}. For the volume averaged normalization one finds $(V_f n_H + V_r \Sigma_i n_i Z_i^2)/(V_f + V_r) \approx 13$ cm^{-3}. Note that both the bremsstrahlung and synchrotron luminosity scale with the emitting volume. It is not unreasonable to assume that the synchrotron emitting volume is equal to the volume of the shock heated plasma. However, it is uncertain how the

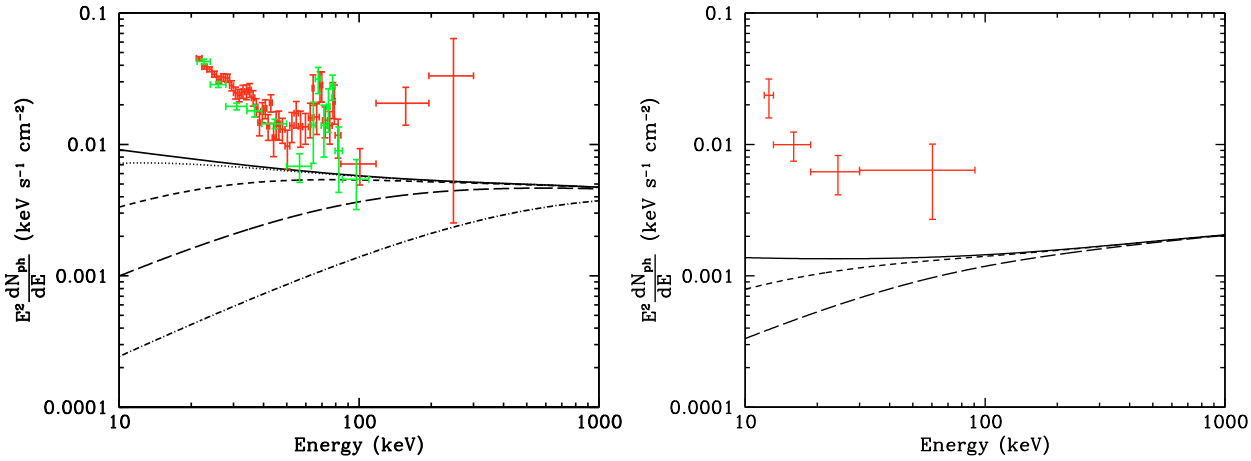

Fig. 3. *Left*: spectral energy distribution of Cas A, as measured with BeppoSAX-PDS (Vink et al. 2001, red) and INTEGRAL-IBIS (Renaud et al. 2006b, green), assuming a magnetic field of ∼300 μG, a spectral energy index of −2.56 (corresponding to a radio-spectral index of $\alpha = -0.78$), and a background plasma with $\Sigma_i \langle n_i Z^2 \rangle = 10$ cm^{-3}. The bremsstrahlung spectra were calculated using the analytic cross sections of Haug (1997). The model spectra are shown for $n_e t = 0, 2\times10^9, 2\times10^{10}, 2\times10^{11}$ and 2×10^{12} cm^{-3} s (*from top to bottom*). *Right*: spectral energy distribution of Tycho's SNR, as measured by the BeppoSAX-PDS. The theoretical curves are for $B = 10$ μG, $\alpha = -0.6$, and $\Sigma_i \langle n_i Z^2 \rangle = 4$ cm^{-3}. The different curves are for $n_e t = 0, 1\times10^{10}, 1\times10^{11}$ cm^{-3} s.

accelerated electron density and magnetic field is distributed over this volume. So the normalization of $\Sigma_i \langle n_i Z_i^2 \rangle = 10$ cm^{-3} used in Fig. 3 should be considered as a reasonable guess. For a constant non-thermal bremsstrahlung emissivity a higher value of $\Sigma \langle n_i Z_i^2 \rangle$ implies a higher magnetic field.

In contrast, for Tycho's SNR, due to its much lower radio luminosity, one only expects a detection of the non-thermal bremsstrahlung, if the magnetic field turns out to be unexpectedly low: $B \lesssim 10$ μG. This is roughly the value of the compressed average ISM magnetic field, whereas estimates for the magnetic field in Tycho indicates $B \sim 300$ μG (Völk et al. 2005).

Finally, one could also consider SNRs in which the densities and $n_e t$ values are modest, and for which also the magnetic fields are low; for example SN1006 ($n_e t = 2\times10^9$ cm^{-3} s, Vink et al. 2003) and the Northeast of RCW 86 ($n_e t \sim 5\times10^9$ cm^{-3} s, Vink et al. 2006). The advantage is that although the bremsstrahlung may be weaker, the low $n_e t$ ensures non-thermal bremsstrahlung at lower photon energies. Unfortunately, both these SNRs have also X-ray synchrotron radiation, which may be hard to distinguish from non-thermal bremsstrahlung. However, with imaging spectroscopy above 10 keV one may isolate regions where non-thermal bremsstrahlung is important and X-ray synchrotron radiation absent. Moreover, high spectral resolution spectra may reveal departures from Maxwellian electron distributions. This type of research will have to wait till the emergence of high resolution, high throughput, X-ray imaging spectroscopy with XEUS (Parmar et al. 2006).

4. Summary and conclusions

I have derived an analytic expression for the low energy electron cosmic ray spectrum, assuming that the cosmic ray spectrum, as produced by the diffusive acceleration process, is a power law in momentum, and is only affected by Coulomb losses downstream of the shock. As may be expected, the parameter governing the Coulomb losses depends on $n_e t$, the product of (background) electron density and the age of the accelerated electron population. This parameter is similar to the ionization time scale of the hot, shock heated plasma, and can be easily estimated from the line spectra of SNRs.

For the SNRs with high densities, and large $n_e t$, one does not expect a large population of accelerated electrons below 100 keV. This is in particular the case for the very bright radio source Cas A. Nevertheless, Cas A remains a good candidate for searching for non-thermal bremsstrahlung, because of its high ion density and because its radio brightness indicates a large amount of accelerated electrons. Based on reasonable, but somewhat uncertain, assumptions, the results presented here imply that only above ∼100 keV one expects to pick up the non-thermal bremsstrahlung component from Cas A. This may be accomplished with future deep Suzaku HXD observations, or additional deep INTEGRAL observations.

Acknowledgements. I am grateful to Prof. Ishida and Dr Bamba for inviting me for a short stay at ISAS, Japan in November 2007. The discussion on Suzaku HXD data of Cas A led to the results reported here. J.V. is financially supported by a Vidi grant from the Netherlands Organization for Scientific Research (NWO).

References

Aharonian, F., Akhperjanian, A. G., Bazer-Bachi, A. R., et al. 2005, A&A, 437, L7
Aharonian, F. A., Akhperjanian, A. G., Aye, K.-M., et al. 2004, Nature, 432, 75
Albert, J., Aliu, E., Anderhub, H., et al. 2007, A&A, 474, 937
Allen, G. E., Keohane, J. W., Gotthelf, E. V., et al. 1997, ApJ, 487, L97
Allen, G. E., Gotthelf, E. V., & Petre, R. 1999, in the Proceedings of the 26th International Cosmic Ray Conference [arXiv:astro-ph/9908209]
Asvarov, A. I., Guseinov, O. H., Kasumov, F. K., & Dogel', V. A. 1990, A&A, 229, 196
Bamba, A., Yamazaki, R., Yoshida, T., Terasawa, T., & Koyama, K. 2005, ApJ, 621, 793
Berezhko, E. G., & Völk, H. J. 2004, A&A, 419, L27
Berezhko, E. G., Ksenofontov, L. T., & Völk, H. J. 2003, A&A, 412, L11
Bykov, A. M., & Uvarov, Y. A. 1999, JETP, 88, 465
Drury, L. O., Duffy, P., Eichler, D., & Mastichiadis, A. 1999, A&A, 347, 370
Ellison, D. C., Decourchelle, A., & Ballet, J. 2004, A&A, 413, 189

Ellison, D. C., Decourchelle, A., & Ballet, J. 2005, A&A, 429, 569
Favata, F., Vink, J., dal Fiume, D., et al. 1997, A&A, 324, L49
Ghavamian, P., Laming, J. M., & Rakowski, C. E. 2007, ApJ, 654, L69
Haug, E. 1997, A&A, 326, 417
Haug, E. 2004, A&A, 423, 793
Helder, E., & Vink, J. 2008, ApJ, accepted, [arXiv:0806:3748]
Huba, J. D. 2002, NRL Plasma Formulary
Kalemci, E., Reynolds, S. P., Boggs, S. E., et al. 2006, ApJ, 644, 274
Koyama, K., Petre, R., Gotthelf, E. V., et al. 1995, Nature, 378, 255
Laming, J. M. 2001a, ApJ, 546, 1149
Laming, J. M. 2001b, ApJ, 563, 828
Lee, R. E., Chapman, S. C., & Dendy, R. O. 2004, ApJ, 604, 187
Liedahl, D. A. 1999, Lecture Notes in Physics (Berlin: Springer Verlag), 520, 189
Malkov, M. A., & Drury, L. 2001, Rep. Progr. Phys., 64, 429
Parizot, E., Marcowith, A., Ballet, J., & Gallant, Y. A. 2006, A&A, 453, 387
Parmar, A. N., Arnaud, M., Barcons, X., et al. 2006, in Proc. SPIE, 6266, 50
Renaud, M., Vink, J., Decourchelle, A., et al. 2006b, ApJ, 647, L41
Sarazin, C. L. 1999, ApJ, 520, 529
Schmitz, H., Chapman, S. C., & Dendy, R. O. 2002, ApJ, 579, 327
Shklovsky, J. S. 1968, Supernovae, Interscience Monographs and Texts in Physics and Astronomy (London: Wiley)
Stage, M. D., Allen, G. E., Houck, J. C., & Davis, J. E. 2006, Nature Phys., 2, 614
Takahashi, T., Abe, K., Endo, M., et al. 2007, PASJ, 59, 35
The, L.-S., Leising, M. D., Kurfess, J. D., et al. 1996, A&AS, 120, C357
Völk, H. J., Berezhko, E. G., & Ksenofontov, L. T. 2005, A&A, 433, 229
Vink, J. 2005, in High Energy Gamma-Ray Astronomy, ed. F. A. Aharonian, H. J. Völk, & D. Horns, AIP Conf. Proc., 745, 160
Vink, J., & Laming, J. M. 2003, ApJ, 584, 758
Vink, J., Kaastra, J. S., & Bleeker, J. A. M. 1996, A&A, 307, L41
Vink, J., Kaastra, J. S., & Bleeker, J. A. M. 1997, A&A, 328, 628
Vink, J., Laming, J. M., Kaastra, J. S., et al. 2001, ApJ, 560, L79
Vink, J., Laming, J. M., Gu, M. F., Rasmussen, A., & Kaastra, J. 2003, ApJ, 587, 31
Vink, J., Bleeker, J., van der Heyden, K., et al. 2006, ApJ, 648, L33
Warren, J. S., Hughes, J. P., Badenes, C., et al. 2005, ApJ, 634, 376
Willingale, R., Bleeker, J. A. M., van der Heyden, K. J., Kaastra, J. S., & Vink, J. 2002, A&A, 381, 1039
Yang, X.-J., Lu, F.-J., & Chen, L. 2007 [arXiv:0712.1071]